

## Supporting Information

### Colloidal quantum-dot-based silica gel glass: Two-photon absorption, emission, and quenching mechanism

Jingzhou Li,<sup>a,b</sup> Hongxing Dong,<sup>\*a</sup> Saifeng Zhang,<sup>a</sup> Yunfei Ma,<sup>c</sup> Jun Wang<sup>a</sup> and Long Zhang<sup>\*a,d</sup>

<sup>a</sup>Key Laboratory of Materials for High-Power Laser, Shanghai Institute of Optics and Fine Mechanics, Chinese Academy of Science, Shanghai 201800, China.

<sup>b</sup>University of Chinese Academy of Sciences, Beijing 100049, China

<sup>c</sup>Laboratory for Advanced Materials, Department of Chemistry, East China University of Science and Technology, Shanghai 200237, People's Republic of China

<sup>d</sup>IFSA Collaborative Innovation Center, Shanghai Jiao Tong University, Shanghai 200240, China

*E-mail: [hongxingd@siom.ac.cn](mailto:hongxingd@siom.ac.cn); [lzhang@siom.ac.cn](mailto:lzhang@siom.ac.cn)*

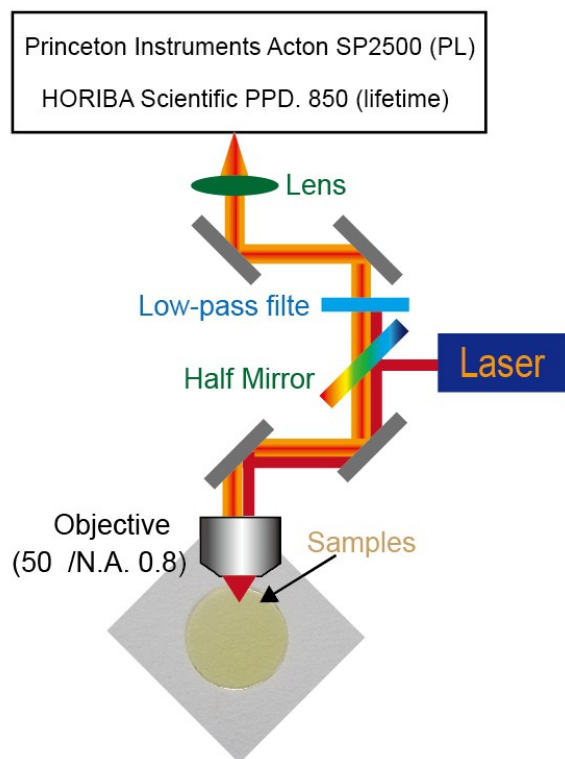


**Fig. S1.** Schematic diagram of the experimental setup used to monitor the TP PL and lifetime.

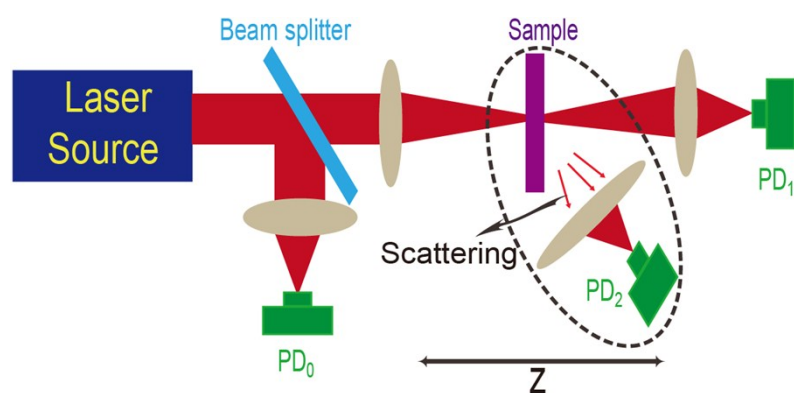


**Fig. S2.** Schematic diagram of the Z-scan setup, where the 340 fs, 1040 nm pump pulse is followed.

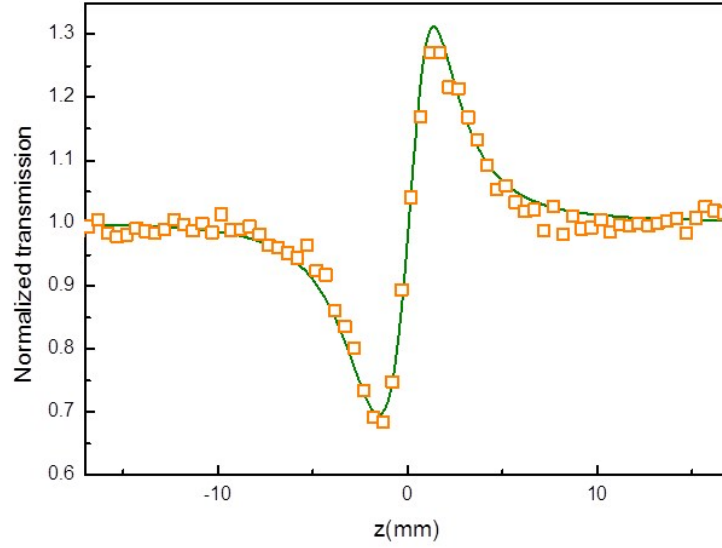


**Fig. S3.** The determination of nonlinear refractive index of the sample (close aperture/open aperture signal). The close aperture signal is divided by open aperture signal to get the nonlinear refractive index. The nonlinear refractive index can be obtained from this equation:

$$n_2 = \left( \frac{\lambda}{2\pi} \right) \frac{\Delta\Phi_0}{I_0 L_{eff}}, \quad |\Delta\Phi_0| = \frac{\Delta T_{pv}}{0.406(1-S)^{0.25}} \quad \text{and} \quad L_{eff} = (1 - e^{-\alpha L})/\alpha.$$
 Here  $\Delta T_{pv}$  is the change in the normalized transmittance between the peak and the valley,  $S$  is the linear transmittance of the aperture without the sample ( $\sim 0.15$  in our experiment),  $L_{eff}$  is the effective thickness of the sample. The nonlinear refractive index  $n_2$  of our sample is about  $1.32 \times 10^{-16} \text{ cm}^2/\text{W}$ .

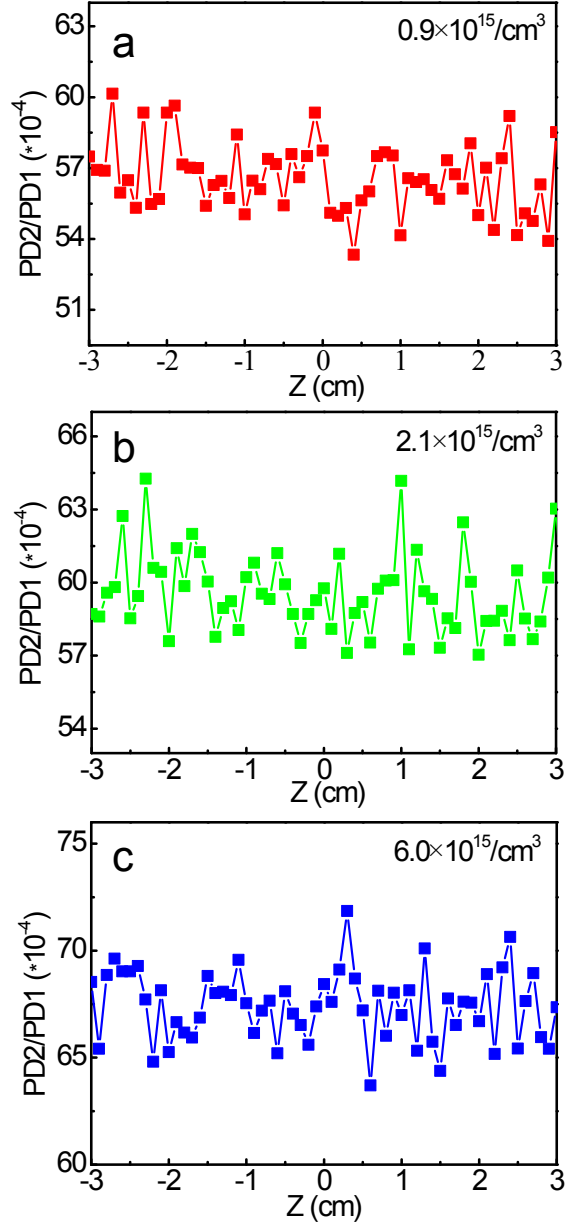


**Fig. S4.** Scattering results of the CQD-SGG with different doping concentrations when carrying out the open-aperture Z-scans experiments with pump pulses at 1040 nm: (a)  $0.9 \times 10^{15}/\text{cm}^3$ , (b)  $2.1 \times 10^{15}/\text{cm}^3$ , and (c)  $6.0 \times 10^{15}/\text{cm}^3$ .

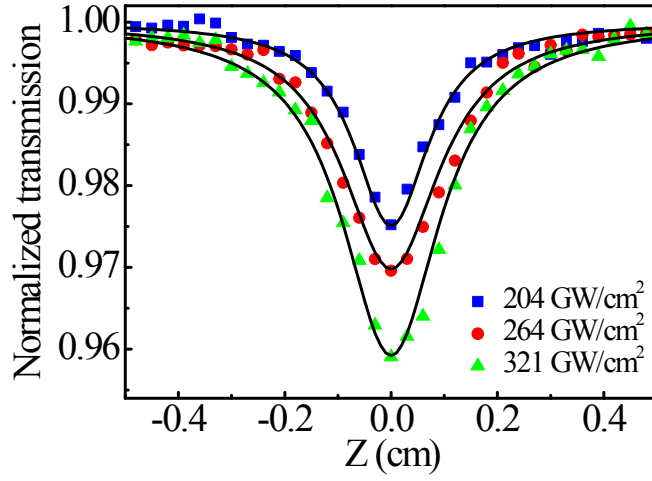


**Fig. S5.** The open-aperture Z-scan results of CQDs in solution under the excitation of 1040 nm. By fitting the results as shown in Fig. S4, we obtained an average value of  $\alpha_{NL} \sim 4.67 \times 10^{-3}$  cm/GW. And, the TPA cross section is calculated as  $\sim 5.0 \times 10^3$  GM. Compared with the results in the silica matrixes, we found that the TP absorption of the two different environments is almost the same.

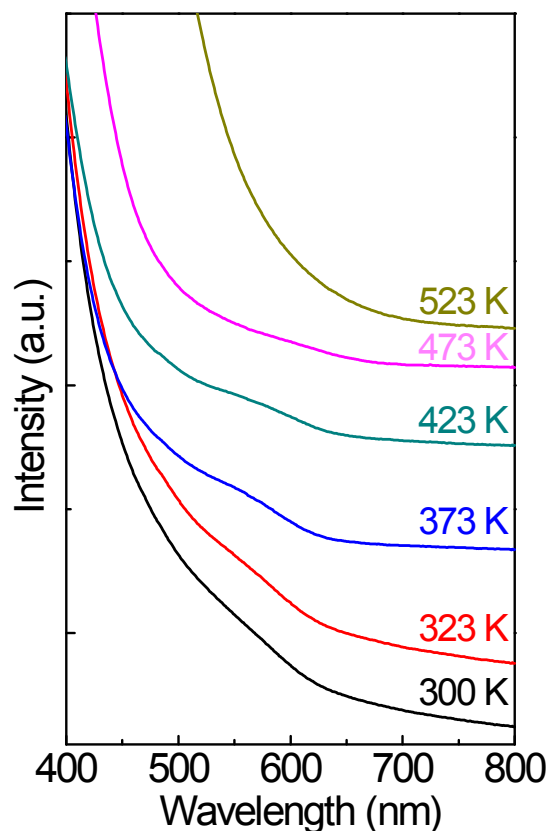


**Fig. S6.** The absorption spectra of the CQD-SGG (the TP PL peak at 609 nm) after heat treatment at different temperatures for 30 min. The absorption spectra of the CQD-SGGs were also recorded after heat treatment at different temperatures for 30 min. The absorption peak of the samples at temperatures lower than 373 K is almost the same (about 571 nm). And the absorption peak at 423 K has a slight red-shift of  $\sim 2$  nm. The results were consistent with the PL spectra (Fig. 4a). With the temperature further increasing, the absorption peaks exhibited an obvious red-shift, and accompanied by broadening. This leads to a red-shift of the PL. This phenomenon is the same as the PL spectra, which can be attributed to the increased defects and the change of the surface environment of the CQDs.

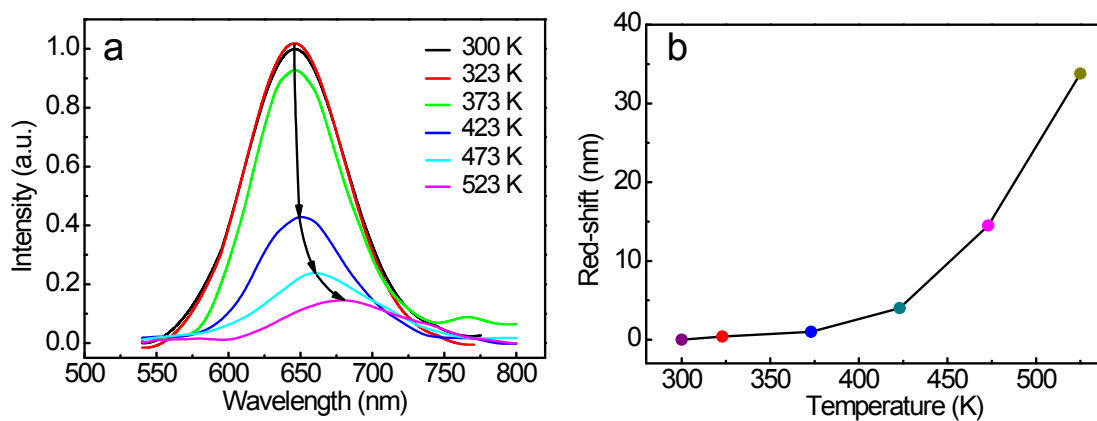


**Fig. S7.** (a) TP PL spectra of the CQD-SGG (the TP PL peak at 646 nm) after heat treatment at different temperatures for 30 min for the same excitation conditions. (b) The red-shift of the emission peak of the samples.



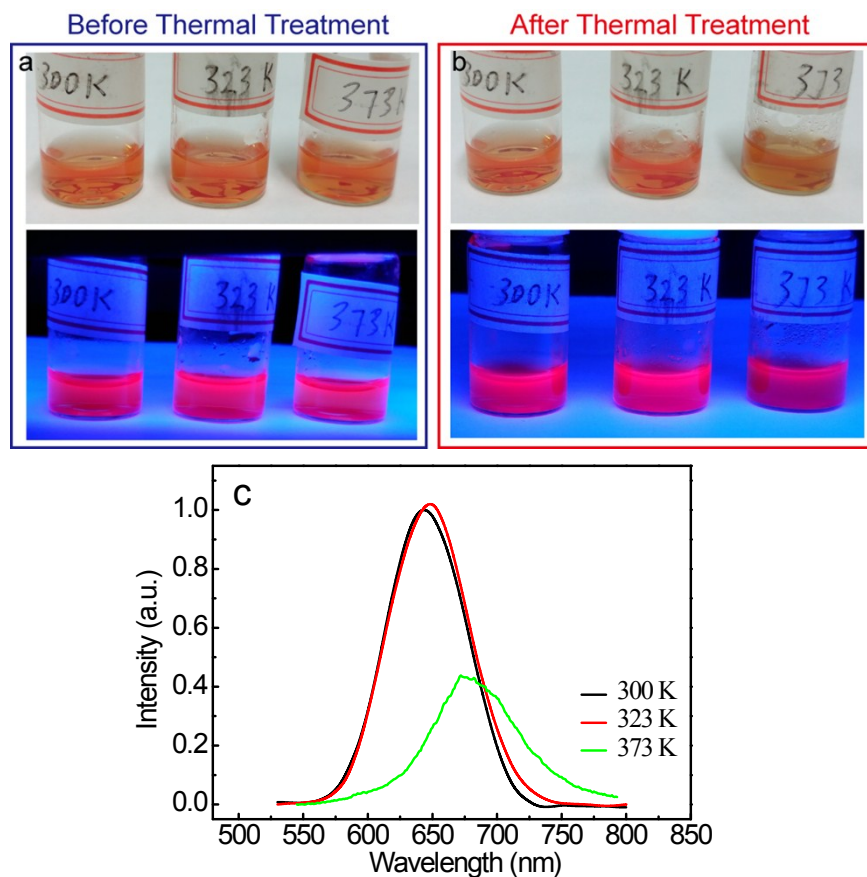


**Fig. S8.** (a, b) Photographs of the CQDs in solution under visible room light (above) and 365 nm UV light (down). a) The solution without thermal treatment. b) The solution after thermal treatment under different temperature (300 K, 323 K, and 373 K). c) The PL spectra of the CQDs in solution after thermal treatment under different temperature. We can found that the PL intensity of the CQDs in solution drop significantly at 373 K (100 °C) with increasing thermal treatment. Compared with the photographs of the CODs that before and after thermal treatment (a, b), the color of the solution at 373 K become dark under visible room light, and brightness dimming under 365 nm UV light. As shown in Fig. 3c, the PL intensity has a slight increase at 323 K, corresponding to a red-shift of ~6 nm. When the treatment temperature increased to 373 K, the PL intensity show a severe degeneration (decrease of about 58%), and the peak have a red-shift of 28 nm. This can be attributed to the Ostwald ripening process.

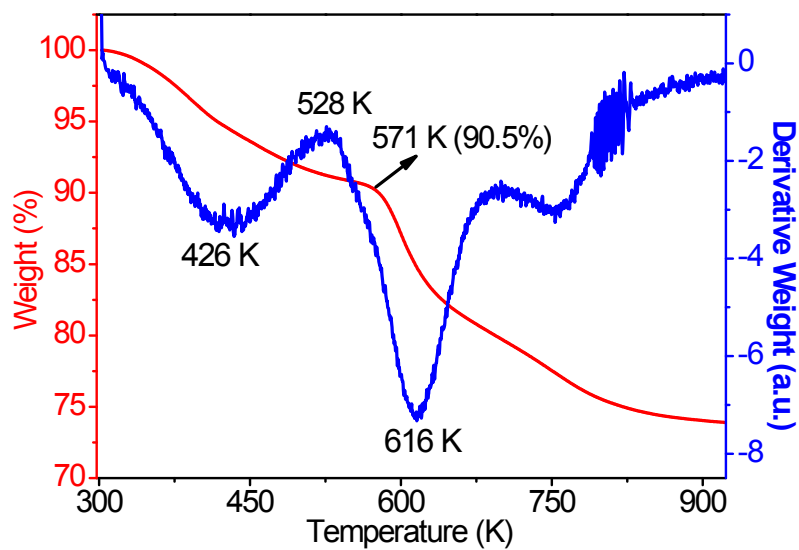


**Fig. S9.** The TGA (red) and DTG (blue) curves of the CQD-SGG samples. TG analysis shows that the mass loss is about 8 wt% in the temperature range of 300–523 K, which are mainly attributed to H<sub>2</sub>O and ethanol. The DTG curves show the weight loss rate is a maximum at 426 K in the temperature range.

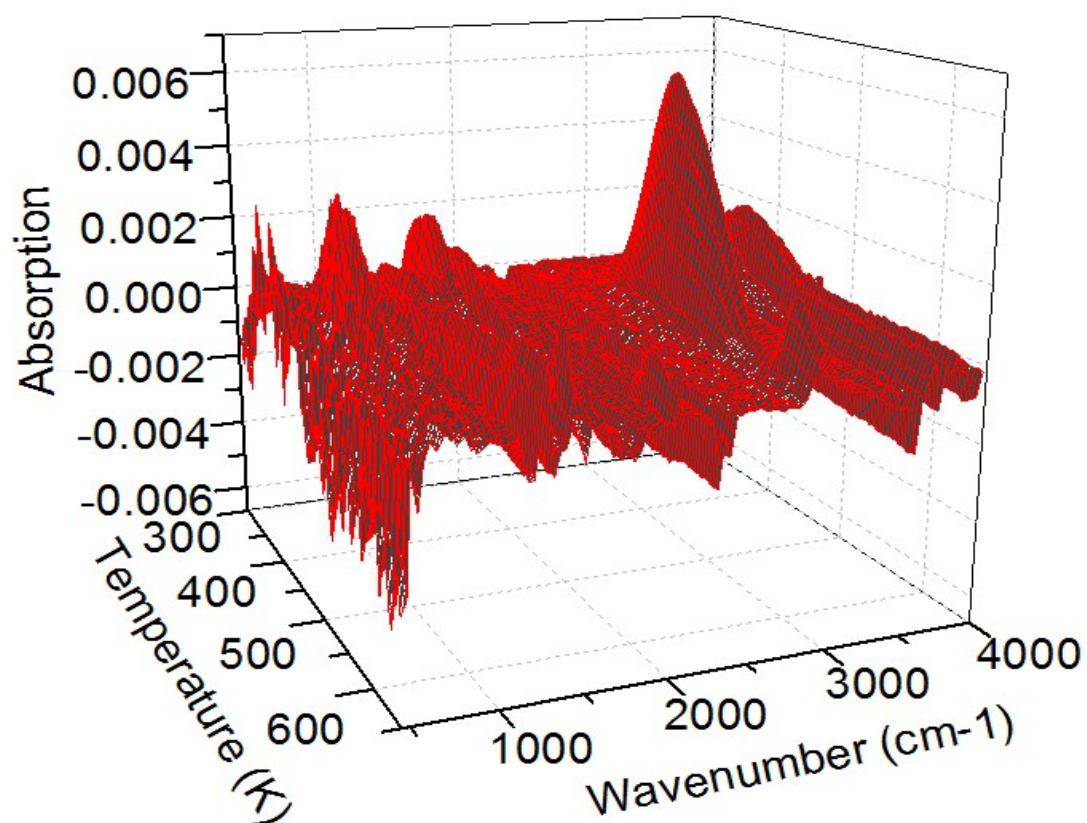


**Fig. S10.** 3D TG-FTIR spectra of the evolved gases from the CQD-SGG. The absorbance peaks are mainly in the regions of 3050–2780  $\text{cm}^{-1}$  and 820–690  $\text{cm}^{-1}$  in the temperature range of 423–523 K, which indicated that the loss weight mainly come from organic molecules (ethanol and propylamine).

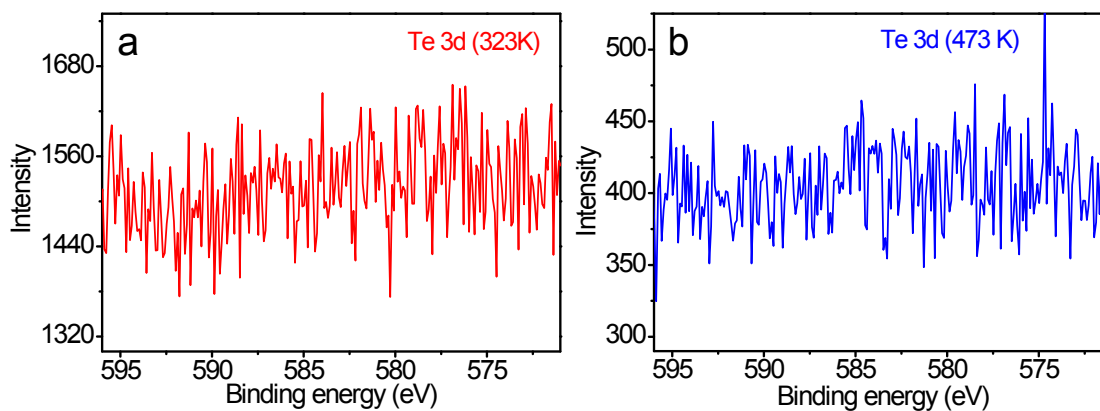


**Fig. S11.** XPS spectra of the Te 3d peaks of the CQD-SGG with thermal treatment temperatures of 323 K (a) and 473 K (b). The Te 3d peaks are located at about 572 eV ( $3d_{5/2}$ ) and 583 eV ( $3d_{3/2}$ ). In our experiments, the Te 3d peaks were not observed, indicating that the XPS signals only detected the surface elements of the CdTe/CdS CQDs.